



**AIIM**

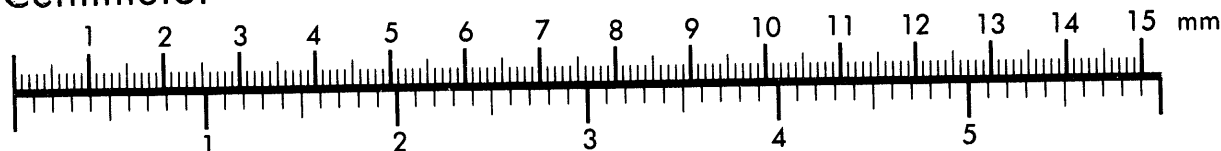
**Association for Information and Image Management**

1100 Wayne Avenue, Suite 1100

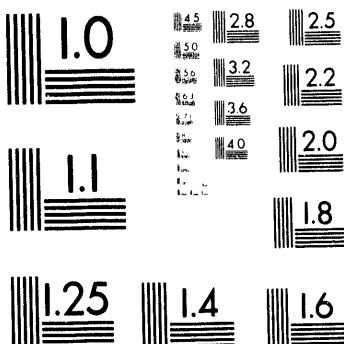
Silver Spring, Maryland 20910

301/587-8202

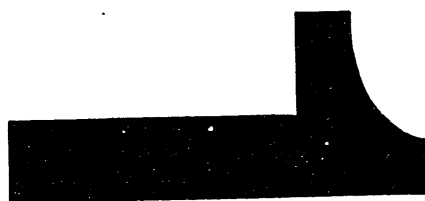
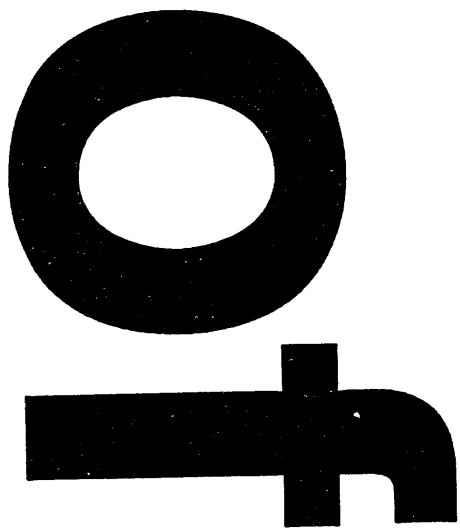
**Centimeter**



**Inches**



MANUFACTURED TO AIIM STANDARDS  
BY APPLIED IMAGE, INC.



Conf-940553-18

2/27/94

SEARCHED - 2/27/94

MODELING HETEROGENEOUS UNSATURATED POROUS  
MEDIA FLOW AT YUCCA MOUNTAIN

REF ID: A6757

MAR 24 1994

OSTI

Thomas H. Robey  
Spectra Research Institute  
1613 University Blvd., NE  
Albuquerque, New Mexico 87102  
(505) 848-0772

## ABSTRACT

Geologic systems are inherently heterogeneous and this heterogeneity can have a significant impact on unsaturated flow through porous media. Most previous efforts to model groundwater flow through Yucca Mountain have used stratigraphic units with homogeneous properties.<sup>1,2</sup> However, modeling heterogeneous porous and fractured tuff in a more realistic manner requires numerical methods for generating heterogeneous simulations of the media, scaling of material properties from core scale to computational scale, and flow modeling that allows channeling. The Yucca Mountain test case of the INTRAVAL project is used to test the numerical approaches. Geostatistics is used to generate more realistic representations of the stratigraphic units and heterogeneity within units is generated using sampling from property distributions. Scaling problems are reduced using an adaptive grid that minimizes heterogeneity within each flow element. A flow code based on the dual mixed-finite-element method that allows for heterogeneity and channeling is employed. In the Yucca Mountain test case, the simulated volumetric water contents matched the measured values at drill hole USW UZ-16 except in the nonwelded portion of Prow Pass.

## I. INTRODUCTION

Geologic systems, such as those containing the potential repository at Yucca Mountain are very complex. Often, geologic interpretation simplifies the representation of the system into a layer-cake of smooth stratigraphic

units. However, the real system contains stratigraphic units that vary in thickness and position within Yucca Mountain in a much more complex manner. Often these complex variations are related to both the depositional and erosional histories of the various units. Tectonic processes further affect the stratigraphic units by faulting and tilting of the units. Basin and Range-style normal faulting is dominant in the Cenozoic section containing the tuffs at Yucca Mountain. These normal faults may consist of sharp offsets or fault zones where the fault consists of many small offsets distributed along a larger lateral distance.

An additional complexity in the system exists due to the internal heterogeneity of each individual stratigraphic unit. Both lateral and vertical heterogeneities occur in the tuffaceous units at Yucca Mountain. The variations can result from many things including changes in the degree of welding, secondary alterations such as zeolitization or devitrification, or fracture density. All of these heterogeneities can influence flow and transport.

Heterogeneity is very much scale-dependent. It is expected that material properties measured on small core samples will exhibit more variation than measurements at larger scales, such as the scale typically used for flow computation. Formulas for scaling are dependent on the particular material property. Even if a good (and efficient) scaling formula is known, the formula only is expected to be accurate on the average and could produce a poor result in a particular case. The result is a great deal of uncertainty in the material properties used in flow calculations. For most properties, the uncertainty in the

This work was supported by the United  
States Department of Energy under  
Contract DE-AC04-94AL85000.

DISTRIBUTION OF THIS DOCUMENT IS UNRESTRICTED

MASTER

EP

properties for a flow element potentially could be as great as the range of the core scale properties found within the flow element.

The complexity of the natural system at Yucca Mountain requires relatively large amounts of data to describe the properties within the system. The proper relationships between the material properties and spatial relationships for each property add to the complexity. It is important to incorporate these relationships if they are significant to flow and transport; however, few of the relationships are well understood. It is not possible to collect enough information to perfectly describe the hydrogeologic system at Yucca Mountain. Therefore analysts require methods for extrapolating and interpolating the available data to arrive at reasonably realistic representations of Yucca Mountain. Geostatistical methods are one of the major tools available to use information on spatial relationships to provide more realistic representations.

Flow codes used to model flow at Yucca Mountain must be designed to handle unsaturated conditions. Modeling unsaturated flow through fractured tuff requires handling a high degree of nonlinearity. Furthermore, in terms of radionuclide containment, the issue of great interest is determining where and when fast paths are formed. One way that fast paths might occur is when fracture coatings prevent liquid flowing in the fractures from being imbibed into the matrix. Another way for fast paths to form is by channeling of unsaturated flow in heterogeneous media. Channeling can produce locally saturated regions that may induce faster flow through the matrix or may result in fracture flow. Models that produce broad saturation fronts; i.e., uniform flow, are not likely to produce fast travel paths. Most flow codes require many nodes at material interfaces or near channeling. Since unsaturated conductivity (a function of saturation) and the location of channeling is unknown *a priori*, such flow codes may not be suitable for modeling flows at Yucca Mountain.

The Yucca Mountain case of the INTRAVAL project is used to test the numerical approaches for heterogeneous unsaturated flow. INTRAVAL is an international cooperative project focusing on evaluation of conceptual

and mathematical models for ground-water flow and transport in the context of performance assessment for geologic repositories for radioactive waste. Phase II of INTRAVAL began in 1990 and was completed in 1993. The INTRAVAL project involves 26 participating parties from 12 countries and 11 field experiments. The Yucca Mountain test case involved five sets of data and five participants. The goal of the Yucca Mountain test case was to examine heterogeneity and moisture migration in unsaturated rock by predicting the moisture content distributions at drill hole USW UZ-16.

## II. GEOSTATISTICAL STRATIGRAPHY

In many models the stratigraphic units are described by straight lines or planes and often are based on just a few drill holes.<sup>1,2</sup> However geologic systems are composed of geologic units with paleo-topographic relief and features. In unsaturated flow, these features may provide points at which lateral flow is forced to flow downward. In contrast, lateral flow in simulations with straight line stratigraphies continues until the lateral boundary is reached where the subsequent behavior is dependent on the boundary condition employed.<sup>1,2</sup> To allow more realism in constructing the hydrogeologic units, geostatistics is employed in this study.

Indicator geostatistics is particularly appropriate for large sites with sparse data such as Yucca Mountain. The geostatistical simulation covers Ghost Dance Fault to Bow Ridge Fault (eastings 171,405.96 to 173,539.56 meters), northings 231,712.11 to 232,169.31 meters, and elevations of 730.00 to 1309.12 meters. The geostatistical grid is 140 x 30 x 190. Horizontal node spacing is 15.24 meters in both directions and the vertical spacing is 3.05 meters apart. 14 drill holes are used to condition the simulation, although there are fewer drill holes in the eastern part of the simulation as shown in Figure 1. The material in the drill holes is categorized as welded, nonwelded (vitric) or zeolitic. The resulting three-dimensional geostatistical simulation then is interspersed layers of the three categories; from the simulation a hydrogeologic unit stratigraphy is constructed. The hydrogeologic units used are the same as used in the Total System Performance Assessment-1993 and are shown in Figure 2.<sup>3</sup> Three realizations of the hydrogeologic unit stratigraphy have

been generated which allows geologic uncertainty to be incorporated into the modeling. The simulations generally show the edge of Ghost Dance Fault on the left hand side of the simulation and an imbricate fault zone located near the center of the simulation. One of the three realizations is shown in Figure 2. Interfingering of units occurs in some of these realizations which is a limitation of the two point statistics employed, although some interfingering of the welded and nonwelded categories is observed in lithologic logs.

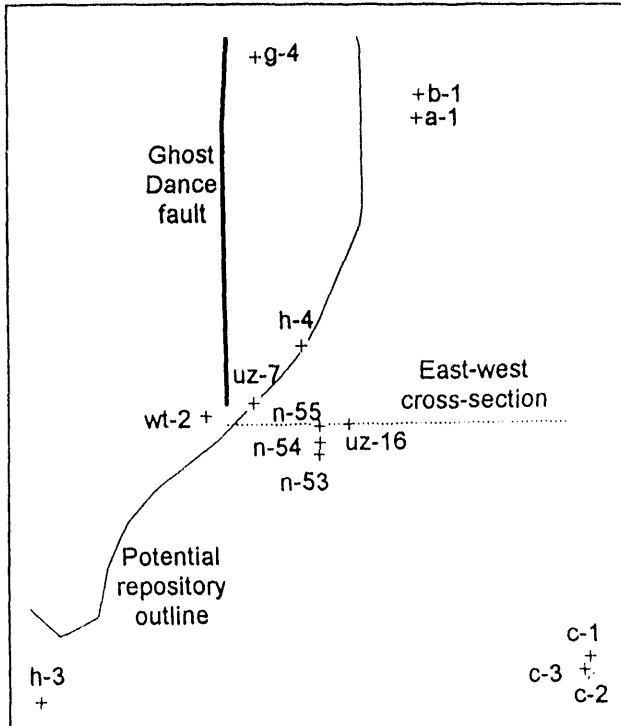


Figure 1: Location of Drill Holes and Cross Section

Porosities are generated for each of the geostatistical nodes by sampling probability distributions based on the hydrogeologic unit to which each node belongs. Smaller features, such as the Topopah Spring basal vitrophyre are added in a deterministic fashion. Spatial correlation or conditioning of porosities is not incorporated since the information likely would be lost in subsequent upscaling.

### III. ADAPTIVE GRID AND SCALING

A two-dimensional cross-section of the porosities is extracted from the geostatistical simulation for use in flow modeling. A relatively coarse flow grid is overlaid on the

finer geostatistical grid. The flow grid should follow the geometrical features in the geostatistical simulation; these features are typically not straight line contacts between the units. It is also important to reduce heterogeneity within flow elements in order to reduce errors in later upscaling of material properties. Both of these objectives are achieved through an adaptive grid.

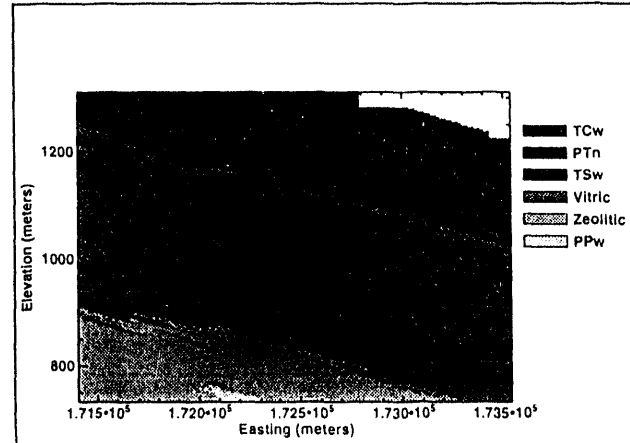


Figure 2: Hydrogeologic Unit Stratigraphy (Seed = 69071)

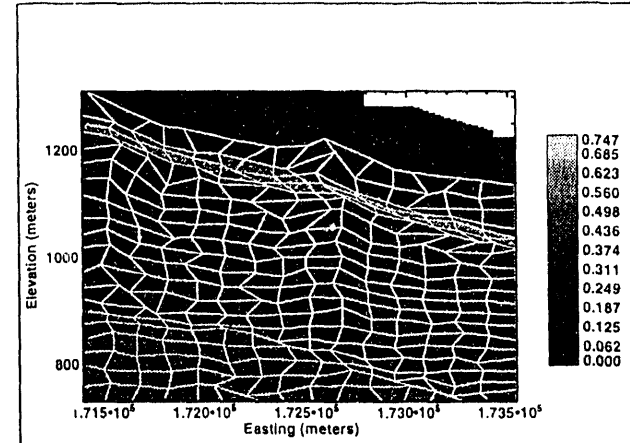


Figure 3: Porosity and Adapted Grid (Seed = 69071)

A measure must be defined to allow different grids to be compared. The 2-norm

$$\|\sigma a\|_2 = \left[ \sum_{i=1}^n (\sigma_i a_i)^2 \right]^{1/2} \quad (1)$$

when used to adapt a grid attempts to make the standard deviation,  $\sigma_i$ , of porosity proportional to the area,  $a_i$ , of the element,  $i$ . This norm can be minimized either by (1)

reducing heterogeneity within elements by aligning the grid with the geometric features, or (2) reducing the size of elements in areas of underlying heterogeneity. Small, heterogeneous elements could be subject to upscaling errors, but presumably the smaller size reduces their importance to the flow calculations. For the three realizations simulated, the average reduction in the 2-norm is 27%. The maximum  $\sigma_i a_i$  is reduced an average of 41%. An example grid is shown in Figure 3.

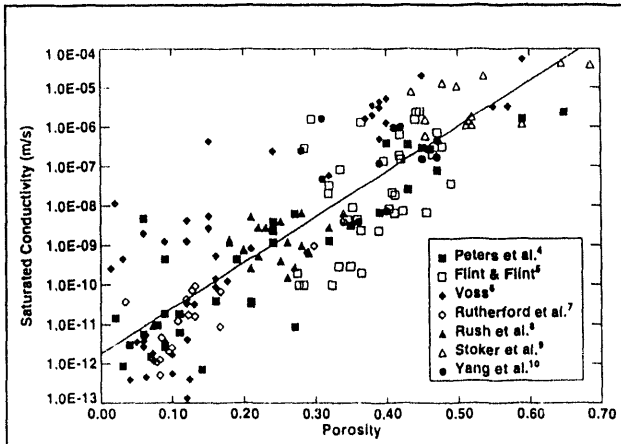


Figure 4: Correlation Between Saturated Conductivity and Porosity for Non-Zeolitic Matrix Materials

Correlations between properties, such as that shown in Figure 4, are used to generate material properties for each geostatistical node based on the porosity and hydrogeologic unit. Once the material properties at the fine scale are known, scaling laws are used to generate the flow element properties. The scaling formula used for porosity is to linearly average all the porosities within an element to obtain an element porosity. For saturated conductivity,  $k_s$ , geometric averaging is used

$$k_s^e = \exp \left[ \frac{1}{n} \sum_{i=1}^n \ln(k_s)_i \right] \quad (2)$$

The gamma function is used for the moisture-retention curve since the gamma parameters correlate with porosity and the gamma function can be easily scaled.<sup>11</sup> The gamma parameters,  $\alpha$  and  $\lambda$ , are related by simple algebraic expressions to the average pore size,  $\bar{r}$ , and the standard deviation of the pore size distribution,  $\sigma(r)$ . Average pore size upscaling uses a volume (porosity) weighted linear averaging

$$\bar{r}^e = \frac{1}{\phi^e n} \sum_{i=1}^n \phi_i \bar{r}_i \quad (3)$$

The standard deviation of the pore size distribution scales using the porosity-weighted parallel axis theorem

$$\sigma(r^e) = \left\{ \frac{1}{\phi^e n} \sum_{i=1}^n \phi_i [\sigma(r_i) + (\bar{r}^e - \bar{r}_i)^2] \right\}^{1/2} \quad (4)$$

#### IV. FLOW SIMULATOR

A nonlinear flow code suitable for heterogeneous systems is required to solve the steady state Darcy flow equation. To date, the primary technique for modeling flow and transport is to use one-dimensional codes where uniform flow is implicitly assumed. Furthermore, introduction of heterogeneity in one-dimensional models is difficult at best.

A dual mixed-finite-element flow code, DUAL, is used for the INTRAVAL test case. The dual mixed-finite-element method has been successfully used in oil reservoir simulation and bioremediation where sharp fronts between fluids are important. Dual mixed finite elements is based upon local conservation of mass across element boundaries while allowing discontinuous saturations (pressures) across element boundaries so that channeling is not suppressed. Introduction of a lateral dimension permits flow around regions of low conductivity. Similarly, two-dimensional flow allows channeling to be modeled. Channeling is important to unsaturated flow because locally saturated regions may result, which allows fast paths and fracture flow. In addition to channeling, the flow code should also be able to handle the highly contorted flow grid.

#### V. RESULTS

The purpose of the INTRAVAL test problem was to predict the volumetric water content at USW UZ-16. The east-west cross-sections extracted from the geostatistical simulations intersect UZ-16 and extend from Ghost Dance Fault to Bow Ridge Fault. The top boundary is the topographic surface and the lower boundary is the water

table. Lateral boundaries are modeled as faults with no flow across them. The lower boundary is taken as the water table with zero pressure. The topographic surface is split into three infiltration zones: alluvium, shaded sideslopes and sunny sideslopes. The three zones are represented respectively by USW UZN-54, USW UZN-53 and USW UZN-55. Each of these drill holes have data on in-situ saturation and porosity. By using an average moisture-retention curve and the top most saturation and porosity, a corresponding pressure can be backed out for use as the top boundary condition.

Figure 5 shows the predictions for volumetric water content at UZ-16 for the three realizations. Also shown is actual volumetric water contents. In the lower part of the drill holes, the simulated volumetric water content does not match the values measured in the nonwelded Prow Pass member. It is apparent that lumping the nonwelded Prow Pass (750 - 780 m) and Calico Hills is the source of the problem. Zeolitic alteration does not appear to be nearly as prevalent in the nonwelded Prow Pass as in the Calico Hills. The Prow Pass is partially welded with the welding varying from nonwelded to moderately welded. Welded tuffs tend to devitrify during initial cooling to stable mineral phases; consequently they tend not to zeolitize. Thus the nonwelded Prow Pass may have sufficient welding to affect secondary alteration to zeolites. Although zeolitic alteration causes only a slight decrease in porosity, it can greatly reduce pore size and saturated conductivity. The smaller pore sizes means a greater capillary suction is required to pull water from the matrix and thus the zeolitic material is more likely to have high saturations. There are also some discrepancies between simulated and measured volumetric water contents, such as in the nonwelded Paintbrush, due to the coarseness of the flow grid.

Saturations for one of the simulations are shown in Figure 6. The saturations in the Topopah Spring member generally reflect the surface infiltration zones. For the shaded sideslope at the left side of the cross section greater saturations occur in the Topopah Spring. Under the central ridge with the sunny sideslope, drier conditions are the result in the Topopah Spring. The velocities for one of the simulations is shown in Figure 7. The velocity plots show considerable lateral flux in the nonwelded

Paintbrush interval. The imbricate fault zone is seen to be somewhat of a barrier to the lateral flow in the nonwelded Paintbrush in all three of the simulations. The velocities below the nonwelded Paintbrush are fairly vertical although the magnitudes vary depending on the saturation of the Topopah Spring member. Exfiltration can be noted where the sunny sideslope boundary is located around the central ridge.

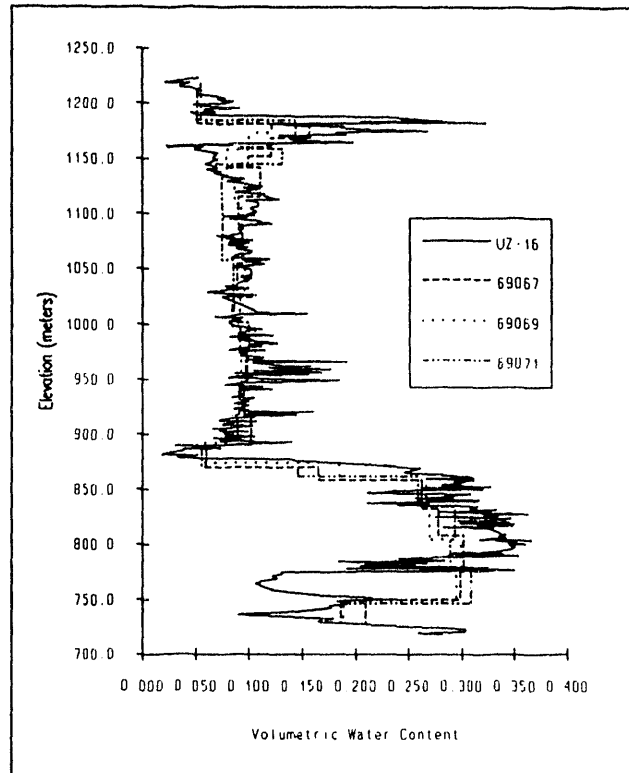


Figure 5: Volumetric Water Contents at UZ-16

In each of three simulations, there are some elements that have regions of local saturation and fracture flow. None of the elements have locally saturated flow throughout the element, which implies that it might be eliminated by finer resolution of the flow grid. Some of the locally saturated elements occur near the nonwelded Paintbrush and may be caused by either offsets in the unit, such as would be expected near the imbricate fault zone, or the interfingering of the welded and nonwelded materials.

## VI. CONCLUSIONS

Numerical methods have been presented that allow heterogeneity to be included into models of unsaturated

porous-media flow in the tuffs at Yucca Mountain. Including heterogeneity increases realism and can potentially uncover fast paths. In this study, lateral flows in the nonwelded Paintbrush are affected by the geometry and heterogeneity and do not continue unimpeded until Bow Ridge Fault (right hand side of the mesh) is reached. In the three simulations, there does not appear to be appreciable channeling, although parts of some of the elements are locally saturated.

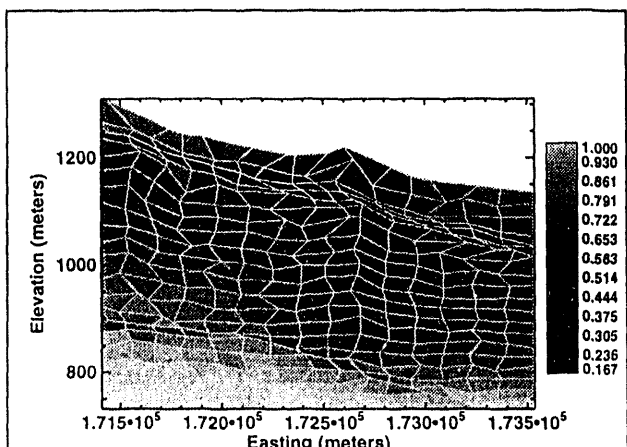


Figure 6: Matrix Saturation (Seed = 69071)

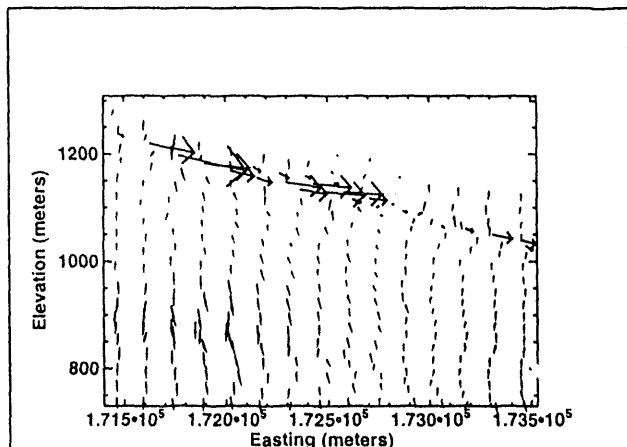


Figure 7: Velocities (Seed = 69071)

The volumetric water contents of the numerical models matched the actual measurements at UZ-16 quite well given the coarseness of the grid. The only poor match is in the nonwelded Prow Pass, indicating that it should be separated from the zeolitic Calico Hills with which it is lumped in this study. . .

## REFERENCES

1. R. W. Prindle and P. L. Hopkins, "On Conditions and Parameters Important to Model Sensitivity for Unsaturated Flow Through Layered, Fractured Tuff: Results of Analyses for HYDROCOIN Level 3 Case 2," *SAND89-0652*, Sandia National Laboratories, Albuquerque, New Mexico, 1990.
2. R. W. Barnard and H. A. Dockery, eds., "Technical Summary of the Performance Assessment Calculational Exercises for 1990 (PACE-90) Volume 1: 'Nominal Configuration' Hydrogeologic Parameters and Calculational Results," *SAND90-2726*, Sandia National Laboratories, Albuquerque, New Mexico, 1991.
3. M. L. Wilson, J. H. Gauthier, R. W. Barnard, G. E. Barr, H. A. Dockery, E. Dunn, R. R. Eaton, D. C. Guerin, N. Lu, M. J. Martinez, R. Nilson, C. A. Rautman, T. H. Robey, B. Ross, E. E. Ryder, A. R. Schenker, S. A. Shannon, L. H. Skinner, W. G. Halsey, J. Gansemer, L. C. Lewis, A. D. Lamont, I. R. Triay, A. Meijer and D. E. Morris, "Total-System Performance Assessment for Yucca Mountain -- SNL Second Iteration (TSPA-1993)," *SAND93-2675*, Sandia National Laboratories, Albuquerque, New Mexico, 1994.
4. R. R. Peters, E. A. Klavetter, I. J. Hall, S. C. Blair, P. R. Heller and G. W. Gee, "Fracture and Matrix Hydrologic Characteristics of Tuffaceous Materials from Yucca Mountain, Nye County, Nevada," *SAND84-1471*, Sandia National Laboratories, Albuquerque, New Mexico, 1984.
5. L. E. Flint and A. L. Flint, "Preliminary Permeability and Water-Retention Data for Nonwelded and Bedded Tuff Samples, Yucca Mountain Area, Nye County, Nevada," *USGS-OFR-90-569*, U.S. Geological Survey, Denver, CO, 1990.
6. C. Voss, "Data Set #1, Yucca Mountain Test Case," *INTRAVAL*, Golder Associates, Inc., Redmond, Washington, 1992.

7. B. M. Rutherford, I. J. Hall, R. R. Peters, R. G. Easterling and E. A. Klavetter, "Statistical Analysis of Hydrologic Data for Yucca Mountain," *SAND87-2380*, Sandia National Laboratories, Albuquerque, New Mexico, 1992.
8. F. E. Rush, W. Thodarson and L. Bruckheimer, "Geologic and Drill-hole Data for Test Well USW H-1, Adjacent to the Nevada Test Site, Nye County, Nevada," *USGS-OFR-83-141*, U.S. Geological Survey, Reston, Virginia, 1983.
9. A. K. Stoker, W. D. Purtymun, S. G. McIn and M. N. Maes, "Extent of Saturation in Mortendad Canyon," *LA-UR-91-1660*, Los Alamos National Laboratory, Los Alamos, New Mexico, 1991.
10. I. C. Yang, A. K. Turner, T. M. Sayre and P. Montazer, "Triaxial Compression Extraction of Pore Water from Unsaturated Tuff, Yucca Mountain, Nevada," *USGS/WRIR-88-4189*, U.S. Geological Survey, Denver, Colorado, 1988.
11. T. H. Robey, "Numerical Methods for Fluid Flow in Unsaturated Heterogeneous Tuff," *High Level Radioactive Waste Management, Proceedings of the Fourth Annual International Conference*, pp. 138-145, American Nuclear Society, La Grange Park, Illinois, and the American Society of Civil Engineers, New York, New York, 1993.

The image consists of three separate, abstract geometric shapes. The top shape is a white rectangle with a black border, centered on a black background. The middle shape is a black rectangle with a white diagonal line from the bottom-left corner to the top-right corner, centered on a white background. The bottom shape is a black U-shaped cutout from a white rectangle, centered on a black background.

DATE  
EDITION  
LIVRE

